Effects of experimental CO_2 enrichment on the PSII photochemical efficiency of *Symbiodinium* sp. in *Acropora millepora*

Ashleigh McNie, Daniel Breen, Kay Vopel *

Department of Environmental Science, School of Science, Auckland University of Technology, Auckland, New Zealand

* Corresponding author

E-mail: kay.vopel@aut.ac.nz

https://doi.org/10.32388/F5CKTW.2

Abstract

Enrichment of seawater with CO_2 decreases the concentration of the carbonate ion while increasing that of hydrogen and bicarbonate ions. We use pulse-amplitude-modulation (PAM) fluorometry to investigate whether, in the absence of warming, and in sub-saturating light, these changes affect the PSII photochemical efficiency of *Symbiodinium* sp. in the reef-building coral *Acropora millepora*. We assessed this experimentally with 30-min-interval saturation pulse analyses at 25 °C, a daily peak in the intensity of the photosynthetically active radiation (PAR) at ~65 µmol quanta m^{-2} s^{-1}, and a seawater pCO_2 that we gradually increased over nine days from ~496 to ~1290 µatm by injection of CO_2-enriched air. Nine 14-day time series, which, except one, were recorded at the growing apices of a coral branch, revealed diel oscillations in the PSII photochemical efficiency characterized by a steep nocturnal decrease followed by a steep increase and peak in the morning, a daily minimum at midday ($\Delta F/F_m'_{,midday}$), and a daily maximum at the onset of darkness at 19:00 h ($F_v/F_{m,19:00\ h}$). An inadvertent shift in the position of one of the PAM fluorometer measuring heads revealed differences between the basal part and the growing coral apices of a coral branch in $\Delta F/F_m'_{midday}$ and Q_m. In ambient seawater (Control) *Symbiodinium* sp. exhibited a gradual decrease, over the course of the experiment, in $\Delta F/F_m'_{,midday}$, $F_v/F_{m,19:00\ h}$, and the slope of the linear regression between the relative electron transport rate and the intensity of PAR (rETR/PAR). Although two of three successive experiments indicated that CO_2 enrichment counteracted these trends, statistical analyses failed to confirm an influence of pCO_2 on $\Delta F/F_m'_{,midday}$, $F_v/F_{m,19:00\ h}$, and Q_m, rendering this experiment inconclusive.

Keywords

CO_2 enrichment; PAM fluorometry; photophysiology; reef-building coral; ocean acidification

Introduction

Enrichment of seawater with CO_2 decreases the concentration of the carbonate ion while increasing that of hydrogen and bicarbonate ions [1]. This shift in the seawater carbonate system occurs in conjunction with ocean warming and can affect coral calcification and photosynthesis, which are intimately coupled [2]. Past experiments have revealed that the coral symbiosis is more susceptible to thermal stress than CO_2 enrichment, and that the physiological plasticity which influences its resilience is species-specific [3–7]. One physiological process of particular interest is the upregulation of the calcifying fluid pH [8,9]. A CO_2 induced increase in seawater $[H^+]$ may increase the energy required for this upregulation [10] and if so, then such additional energy demand must be compensated by photosynthesis of the symbiotic dinoflagellates, which provide most of the coral's energy by transferring photosynthetic products to their hosts [11].

Coral species apparently differ in their photosynthetic response to CO_2 enrichment due to a host-specific regulation of the symbionts' carbon concentrating mechanism (CCM) [12,13]. The CCM uses active bicarbonate transport and carbonic anhydrase to increase the concentration of CO_2 at the site of type II RuBisCO—an enzyme with a low affinity for CO_2 (14–18]. A high carbonic anhydrase activity may indicate that the coral symbiont lives in a carbon-scarce environment and therefore invests energy in concentrating carbon [13]. In *Porites porites* (Pallas, 1766) and *Acropora* sp., enrichment of their environment with CO_2 may then increase the gain from photosynthesis for the benefit of the holobiont [19].

In *Acropora muricata* (Linnaeus, 1758), for example, under conditions of sub-saturating light, CO_2 enrichment can increase chlorophyll pigments and the de-epoxidation of xanthophylls, thus increasing the capacity of the symbiont to photoacclimate to low irradiance [20]. The species *Stylophora pistillata* Esper, 1797 responded similarly with an increase in the concentration of chlorophyll pigments and a corresponding increase in photosynthetic

efficiency [21], and the symbionts in *A. millepora* (Ehrenberg, 1834) and *Seriatopora hystrix* Dana, 1846 apparently increase their maximum PSII quantum yields and light-limited electron transport rates in response to CO_2 enrichment [22].

Other studies support the view that corals do not respond to CO_2 enrichment [23–26], and yet others have demonstrated negative effects. Kaniewska et al. [27], for example, suggested that in *A. millepora*, CO_2 enrichment caused widespread changes in gene expression consistent with metabolic suppression, an increase in oxidative stress, apoptosis and symbiont loss, and a decrease in respiration and photosynthesis. Furthermore, Edmunds [28] reported negative effects of CO_2 enrichment—in this study, CO_2 enrichment decreased both the symbiont's maximum and effective photochemical efficiencies.

Here, we follow the studies by Edmunds [28], Hoadley et al. [25], and Noonan and Fabricus [22], asking if, in the absence of warming, CO_2 enrichment affects the PSII photochemical efficiency of *Symbiodinium* sp. in the reef-building coral *A. millepora*. To investigate this experimentally, we conducted time series of saturation pulse analyses (pulse-amplitude-modulation fluorometry) monitoring the symbiont's maximum photochemical efficiency, F_v/F_m, midday effective photochemical efficiency, $\Delta F/F_m'$, and the relationship between the relative electron transport rate and the intensity of the photosynthetically active radiation (rETR/PAR) while gradually increasing the seawater pCO_2.

Material and methods

Experimental design

We conducted three consecutive laboratory experiments in each of which we acclimated one fragment (~7 cm tall, 4 cm wide) of the coral *A. millepora* for seven days in each of three seawater recirculation tanks to a simulated daily light cycle that peaked midday at a photosynthetically active radiation (hereafter, PAR) of ~65 μmol quanta m^{-2} s^{-1} (Fig 1, S1 Fig

1). The nine coral fragments originated from one large *A. millepora* specimen collected off the East Coast of Australia, and therefore, we assume that they hosted the same *Symbiodinium* clade.

After their collection, and until acclimation in the laboratory, the coral fragments were kept under a constant 12/12 h dark/light regime (PAR ~ 90 μmol quanta m^{-2} s^{-1}, Kessil A160WE Tuna Blue LED). In the laboratory, they were placed on a gridded plate under the measuring head of a pulse-amplitude-modulation (PAM) fluorometer (Monitoring-PAM aquatic version, Walz GmbH, Germany) and a Kessil A80 Tuna Blue controllable LED (S1 Figs 1, 2). Because only three PAM fluorometer measuring heads were available for this study, three sets of three time-series measurements were conducted consecutively. For a recent review of the strengths and limitations of chlorophyll fluorescence measurement, see Bhagooli et al. [29].

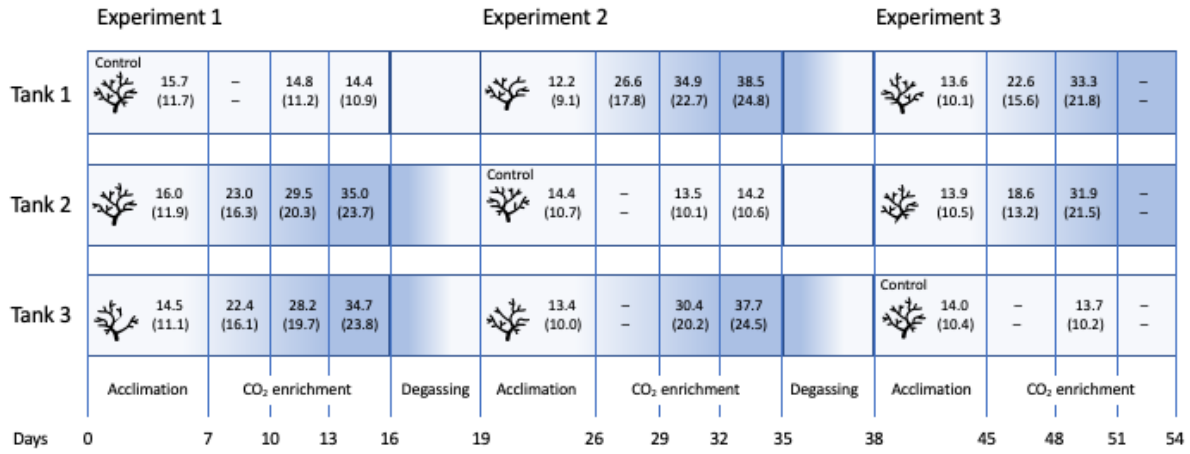

Fig 1. Experimental design and timeline. In each of three consecutive 16-day experiments, one coral fragment was tested in each of three tanks. Transitions from white to blue shades indicate an increase in seawater pCO_2. Numbers, seawater [CO_2] at 25 °C (μmol kg^{-1}); numbers in parentheses, seawater [H^+] at 25 °C (nmol L^{-1}). N-dashes indicate missing data.

Following 7 days of acclimation, the seawater pCO_2 was gradually raised and then maintained in two of the three tanks from ~500 to ~1200 μatm by computer-controlled injection of CO_2-

enriched air over the next nine days in three steps. Computer feedback control adjusted CO_2 additions to target pH values, and the three steps resulted in pH = 7.8 on day 10, pH = 7.7 on day 13, and pH = 7.6 on day 16. In each experiment, one of the three tanks remained at ambient pH = 8.0 (Control). Once the first experiment was completed, the CO_2 injection was shut off, allowing the pCO_2 in seawater and atmosphere to equilibrate before starting the next experiment on day 19 with three new coral fragments. These steps were repeated before starting Experiment 3 on day 38 (Fig 1).

Laboratory setup

Each experimental tank (S1 Fig 1) contained ~450 L seawater collected from Okahu Bay, New Zealand. A submerged pump (1260, Eheim) moved ~9 L min^{-1} from the main tank (112 × 72 × 60 cm) through a water cooler (HC-300A, Hailea) and UV sterilizer (Pond One UV-C 9W, ClearTec) into an elevated mixing barrel (210 L) from which the seawater returned to the main tank by gravity. The sizes of the tank and mixing barrel, and the flow rate of the pump, were chosen to ensure that short-term fluctuations in the pCO_2 of the seawater in the mixing barrel (due to CO_2 enriched air injection, as explained below) did not affect the tank.

A heater (500 W GH Quartz Glass heater, Aqua One) was placed at the floor of the main tank. The chiller and heater maintained the seawater temperature at 25 ± 0.5 °C. The seawater was also pumped from the main tank through an external particle filter (Professional 4+ 350 Cannister filter, Eheim) into a small, elevated plastic container (30 × 20 × 10 cm) that contained the coral fragment. The tube returning seawater from the particle filter was aimed towards the coral fragment to ensure rapid flow across the coral surface. The overflow from this container returned the seawater into the main tank.

The distance between the measuring head of the PAM fluorometer and the coral surface was ~40 mm. The PAM fluorometer measures ambient light immediately adjacent to the area under test using a small sheet of Teflon placed flush with the measured tissue and reflecting

light to an internal PAR sensor. This sensor was calibrated against a Li-Cor Li-192 underwater quantum sensor. The PAM recordings show that the LED mounted above each coral fragment gradually increased the intensity of PAR from 5 am to a midday maximum of ~65 µmol quanta m^{-2} s^{-1} and then gradually decreased this intensity until 7 pm, when the LED was turned off (S1 Fig 2). Note that the lowest irradiance emitted from the LED was ~20 µmol quanta m^{-2} s^{-1}. The resulting daily flux, as measured by the internal PAR sensor of the PAM fluorometer, ranged between 1.7 and 2.6 mol quanta m^{-2} day^{-1}.

Saturation pulse and induction/recovery analyses

The Walz software WinControl-3.0 ran a batch routine to automatically perform one saturation pulse analysis every 30 minutes between 03:00 and 24:00 h and one daily induction/recovery analyses between 02:00 and 02:30 h. The following settings were applied: saturation pulse intensity = 12, saturation pulse width = 0.6 s, gain = 1, measuring light intensity = 6, measuring light frequency = 3. The measuring light was turned off between saturation pulses and initial measurements of the baseline florescence confirmed that the intensity of the measuring light did not cause an actinic light effect. The daily induction/recovery analyses started with an F_0 determination, followed by a series of 12 saturation pulses (delay = 40 s) 20 seconds apart with the actinic light on (65 µmol quanta m^{-2} s^{-1}). After ~4 minutes, the actinic light was turned off, and a series of 8 saturation pulses occurred at increasing intervals between 0.5 and 9 minutes. Prior to deployment, each PAM sensing head was zeroed in the experimental setup.

We derived the maximum PSII photochemical efficiency, F_v/F_m, from measurements of F_0 and F_m in darkness: $F_v/F_m = (F_m – F_0)/Fm$ (Table 1) [30]. The effective photochemical efficiency, $\Delta F/F_m'$, was derived from the maximum (F_m') and minimum (F') fluorescence yields at ambient light intensity: $\Delta F/F_m' = (F_m' – F') / F_m'$ [30]. F_v/F_m measured at 19:00 h, and $\Delta F/F_m'$ measured at midday gave the midday excitation pressure, Q_m: $Q_m = 1 – [(\Delta F/F_m'_{,midday}) /$

($F_v/F_{m,19:00\ h}$)] [31]. The PAR recorded by the internal sensor of the PAM and the effective photochemical efficiency, ΔF/Fm', were used to derive the relative electron transport rate: $rETR = \Delta F/F_m' \times PAR \times 0.5$ [32].

Table 1. Summary of fluorescence parameters measured or derived in conditions of darkness or actinic light. AL, actinic light; SP, saturation pulse.

Symbol	Fluorescence parameter	Equation/comments	Reference
Darkness, measured variables			
F_0	Minimum fluorescence		
F_m	Maximum fluorescence	Saturation pulse	
Darkness, derived variables			
F_v	Variable fluorescence	$F_v = (F_m–F_0)$	
F_v/F_m	Maximum photochemical efficiency	$F_v/F_m = (F_m–F_0)/F_m$	[30]
Actinic light, measured variables			
F_m'	Maximum fluorescence yield	Saturation pulse	
F_0'	Minimum fluorescence yield		
Actinic light, derived variables			
F_v'	Variable fluorescence	$F_v' = (F_m'–F_0')$	
$\Delta F/F_m'$	Effective photochemical efficiency	$\Delta F/F_m' = (F_m'–F')/F_m'$	[30]
Q_m	Excitation pressure	$Q_m = 1 – [(\Delta F/F_{m,'midday})/(F_v/F_{m,\ 19:00\ h})]$ (F_v/F_m measured at 19:00 h, F_m' measured midday)	[31]
rETR	Relative electron transport rate	$rETR = \Delta F/F_m' \times PAR \times 0.5$	[54]

Seawater carbonate system

The pH of the seawater in the mixing barrel of each circulation unit was continuously measured with a SenTix HWD electrode connected to a pH 3310 meter (WTW). These measurements were sent to a computer with CapCtr software (Loligo® Systems ApS) controlling the opening and closing of a solenoid valve when the seawater pH increased above or decreased below the daily set point. The solenoid valve released CO_2-enriched air (5% CO_2, 21% O_2 in nitrogen) from a gas cylinder to a perforated tube in the mixing barrel. The pH electrodes were calibrated using NIST/DIN pH buffers to test for theoretical Nernstian electrode behavior and then conditioned in seawater before determining the electrode-specific offset between the potential measured in NIST/DIN pH buffer and that measured in certified

seawater reference material (TRIS in synthetic seawater). The electrodes were recalibrated at the start of each experiment.

Determination of seawater DIC, TA and salinity

To determine the seawater carbonate system, we collected a one-liter sample from each circulation unit at the start of each experiment, each night before CO_2-enriched air injection was increased, and at the end of the experiment. These samples were preserved with mercuric chloride and later analyzed for dissolved inorganic carbon (DIC) with a SOMMA (Single Operator Multiparameter Metabolic Analyzer) coulometer system and for total alkalinity (TA) with a closed-cell potentiometric titration system following the SOP's 2 and 3a procedures [33]. We used these DIC and TA measurements and D. Pierrot's adaptation of the CO2Sys.BAS program [34] to compute the seawater pCO_2 and pH (total scale, mol kg-SW^{-1}). The dissociation constant for HSO_4^- was taken from Dickson [35]; the values of K1 and K2 of carbonic acid were from Mehrbach et al. [36] refitted by Dickson and Millero [37]. Note that water samples were not collected on the final day of Experiment 3 due to a COVID-19 pandemic lockdown, and four seawater samples were destroyed during transport to the analytical lab (missing data in Fig 1 and S1 Table 2). The seawater salinity was measured with a handheld conductivity meter (Knick, Germany) and maintained at 34.5 ± 0.5 by daily addition of ultrapure water.

Statistical analysis

Although saturation pulse analyses were conducted every 30 minutes, we only used the data collected during the last day of each step-pCO_2 increase (days 7, 10, 13, 16), considering that during this day, conditions in the experimental tanks had been fully established as per the pH set point.

The daily induction/recovery routines were used to assess the effects of CO_2 enrichment on the PSII efficiency using two variables: the variable fluorescence, F_v, determined by analysis of the first saturation pulse of the induction, and the average of the plateaued F_v measured during recovery.

All statistical analyses were performed with R statistical software (version 1.3.959). The Shapiro-Wilk test was used to assess if the data were normally distributed, and homogeneity of variance was tested with the Levenes test. The $F_v/F_{m,19:00\ h}$, $\Delta F/F_m'_{,midday}$, Q_m, and the slope of the linear regression of rETR versus incident PAR were analyzed with a four-factor, nested ANOVA in which individual coral fragments were the random factor nested in tank, treatment, and day of measurement, which were fixed factors. The same ANOVAs were then used to analyze the variables derived from the induction and recovery analyses. We used an Akaike information criterion model selection to determine the best model possible to describe the relationship between the fluorescence parameters, the three tanks, the treatment, and the individual coral fragment. The tank effect was not significant and was removed from the model.

Results

Seawater CO_2 enrichment

The measured and derived seawater carbonate chemistry parameters at the start of each of three consecutive CO_2 enrichment experiments (days 7, 26, and 45; Fig 1) and 3, 6, and 9 days later are summarized in Figure 1 and S1 Table 2. The CO2Sys.BAS computations confirmed that the stepwise increase in the injection of CO_2-enriched air increased the pCO_2 of the ambient seawater in the tanks of the Treatments from 493 ± 44 µatm (n = 6) to 799 ± 101 µatm (n = 5, days 10, 29, and 48), 1109 ± 89 µatm (n = 6, days 13, 32, and 51), and 1290 ± 69 µatm (n = 4, days 16, 35, and 54; S1 Table 2).

Saturation pulse analyses

Time series of saturation pulse analyses revealed diel oscillations in the PSII photochemical efficiency of *Symbiodinium* sp. characterized by a steep nocturnal decrease followed by a steep increase and peak in the morning, a daily minimum at midday, and a daily maximum at the onset of darkness at 19:00 h (Fig 2, S1 Fig 3). We note that the F_v/F_m times series in Fig 2 and S1 Fig 3 were interrupted at 02:00 h by photosynthesis induction routines.

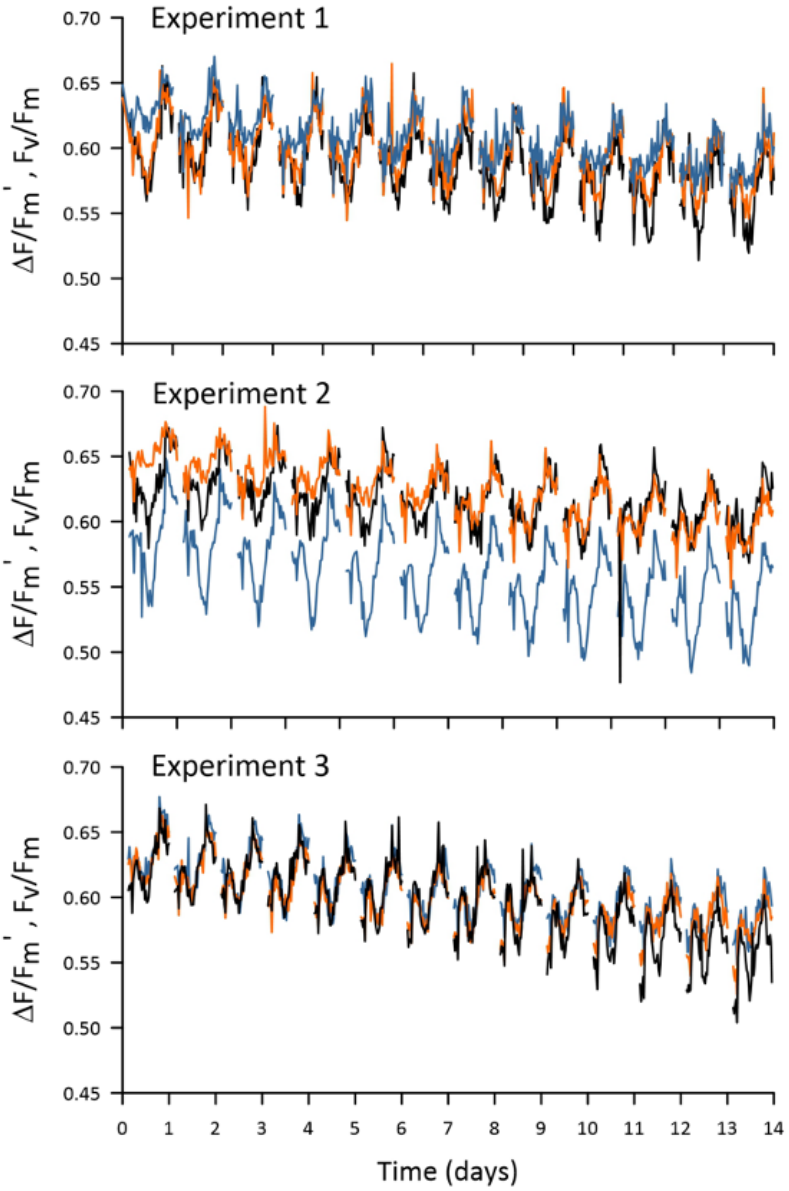

Fig 2. *Symbiodinium* sp. in *Acropora millepora*. Diel variations in the PSII photochemical efficiency (darkness: F_v/F_m; light: $\Delta F/F_m$', see Table 1) of nine coral fragments, one

placed in each of three tanks (tank 1, blue; tank 2, black; tank 3, orange) for each of three consecutive experiments. Daily induction and recovery analyses caused gaps in time series from midnight to 03:00 h.

Both variables, the maximum PSII photochemical efficiency ($F_v/F_{m,19:00\ h}$ recorded at 19:00 h, Table 1) and the midday effective PSII photochemical efficiency, $\Delta F/F_m'_{,midday}$, gradually decreased over the course of the experiment in both Controls and Treatments (Fig 3). This decrease, which produced a significant effect on days 13 and 16 (S1 Table 1), was independent of CO_2 enrichment. Similarly, the midday excitation pressure, Q_m, which was derived from $F_v/F_{m,19:00\ h}$ and $\Delta F/F_m'_{,midday}$ (Table 1), was not affected by CO_2 enrichment (Fig 3, S1 Table 1).

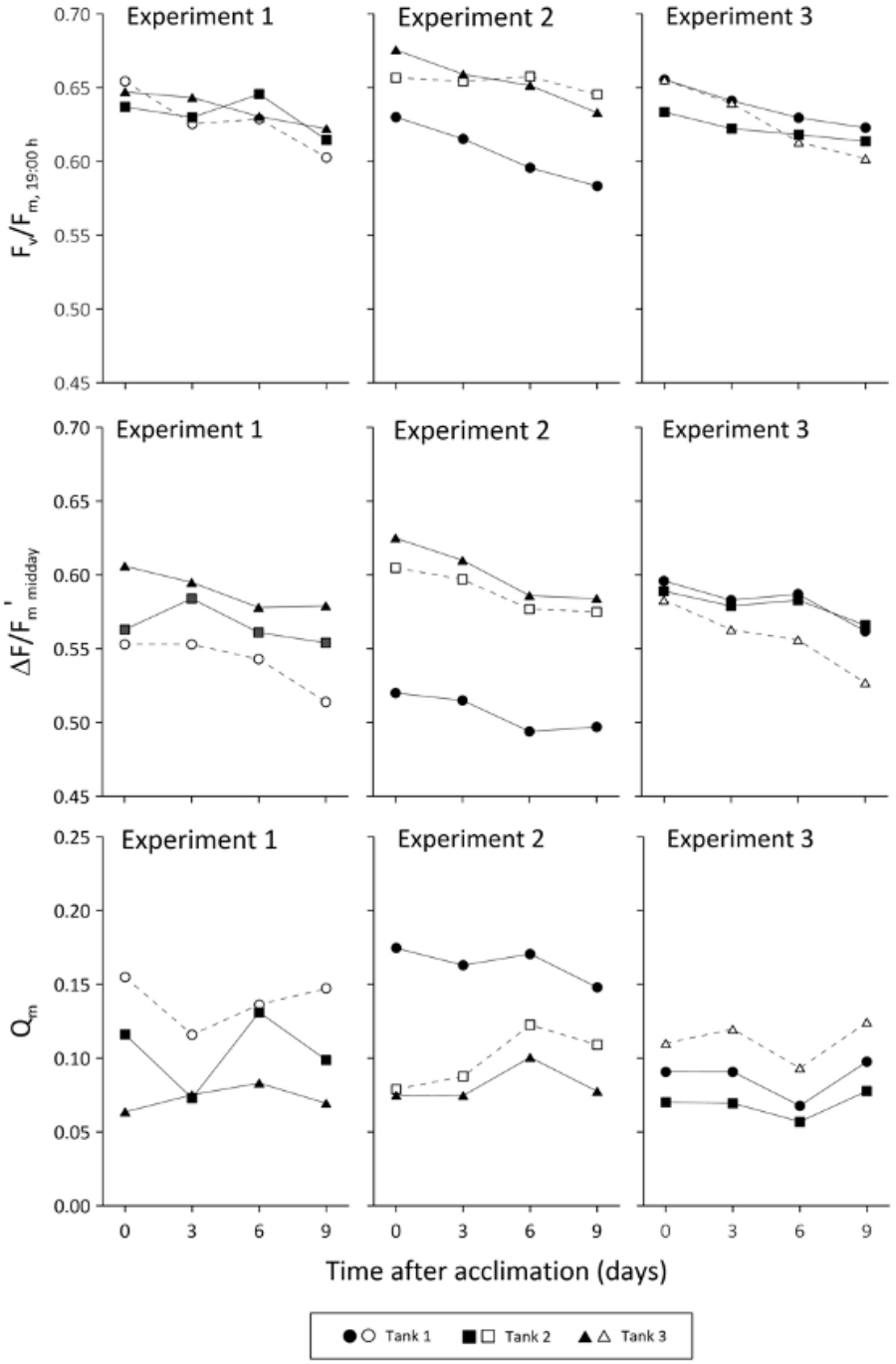

Fig 3. *Symbiodinium* sp. in *Acropora millepora*. Time series of the maximum PSII photochemical efficiency measured at 19:00 h, $F_v/F_{m,19:00\ h}$, the midday PSII effective photochemical efficiency, $\Delta F/F_m'_{,midday}$, and the midday excitation pressure, Q_m (see Table 1), of nine coral fragments, one placed in each of three seawater circulation units (circles, Tank 1; squares, Tank 2; triangles, Tank 3) in each of three consecutive experiments. In each experiment, the seawater in two tanks (filled symbols) was

gradually enriched with CO_2 (Treatment). The pCO_2 in the third unit (open symbols) remained at ~506 µatm over the duration of the experiment (Control).

Our measurements on the coral fragment in Tank 1 of Experiment 2 (Treatment, Fig 1) differed from all other measurements in that the PAM measuring head accidently changed its position so that it was not directed toward the distal but a more basal part of a coral branch. This apparently resulted in much lower PSII photochemical efficiencies (Fig 3). Because the difference in $\Delta F/F_m'_{,midday}$ was greater than that in $F_v/F_{m,19:00\ h}$, the derived Q_m exceeded that of the other two coral fragments tested in Experiment 2 (Fig 3).

The slope of the linear regression between rETR and PAR ($R^2 > 0.997$, S1 Fig 4) decreased over the course of the experiment under ambient pCO_2 conditions (Fig 4, open symbols). Such decrease was also observed in CO_2-enriched seawater (Fig 4, closed symbols), but in Experiments 1 and 3, this decrease was less steep so that the difference in slope between the Control and Treatments increased over the course of the experiment.

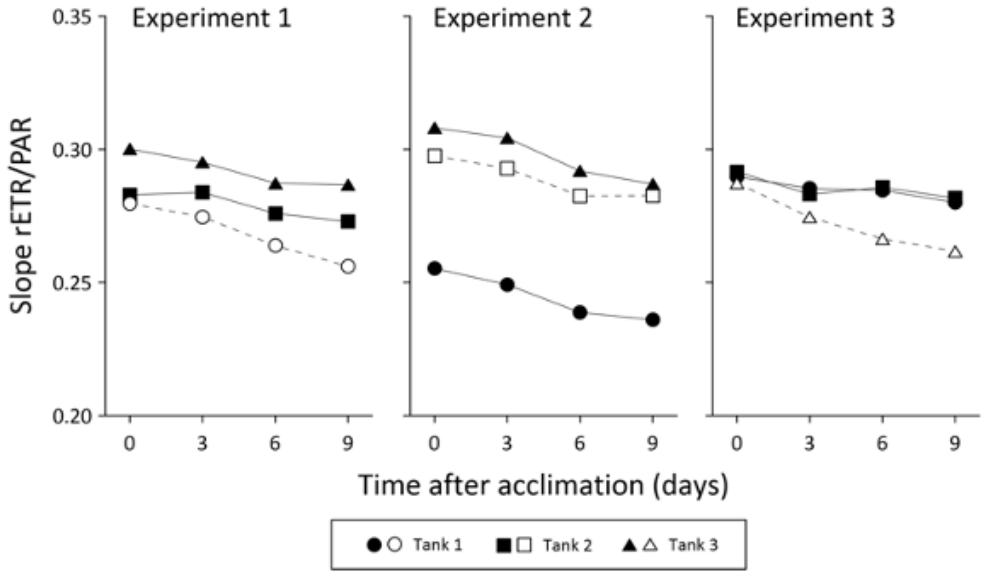

Fig 4. *Symbiodinium* sp. in *Acropora millepora*. Time-series of the slope of the linear regression of relative electron transport rate (rETR) versus incident photosynthetically active radiation (PAR, µmol quanta m^{-2} s^{-1}) shown in S1 Fig 4. The rETR was derived

from measurements immediately after (day 0) and three, six and nine days after acclimation of nine coral fragments, one placed in each of three seawater tanks (circles, tank 1; squares, tank 2; triangles, tank 3) for each of three consecutive experiments. In each experiment, the seawater in two tanks (filled symbols) was gradually enriched with CO_2 (Treatment, see text and S1 Table 2).

Induction–recovery dynamics

Like $F_v/F_{m,19:00\ h}$ and $\Delta F/F_m'_{,midday}$, the variable fluorescence, F_v, recorded during the induction–recovery routine decreased over the course of the experiment in both the Control and Treatment groups (S1 Table 3). F_v measured at the beginning of each nocturnal photosynthesis induction was not affected by CO_2 enrichment (S1 Table 3, S1 Fig 5). Once the actinic light was switched off, F_v gradually recovered, approaching pre-light exposure values (F_v between 600 and 800) within 40 min (S1 Fig 5). Again, CO_2 enrichment did not affect the average postinduction recovery F_v (S1 Table 3, S1 Fig 5).

Discussion

We observed that in ambient seawater (Control) under conditions of a sub-saturating diel light cycle and ~25 °C, *Symbiodinium* sp. exhibited a gradual decrease, over the course of the experiment, in the midday and maximum PSII photochemical efficiency ($\Delta F/F_m'_{,midday}$ and $F_v/F_{m,19:00\ h}$), and the slope of the linear regression between the relative electron transport rate and the intensity of PAR (rETR/PAR). Although two of three successive experiments indicated that CO_2 enrichment counteracted these trends, statistical analyses failed to confirm an influence of pCO_2 on $\Delta F/F_m'_{,midday}$, $F_v/F_{m,19:00\ h}$, and the midday excitation pressure, Q_m, rendering this experiment inconclusive.

The midday excitation pressure, Q_m, is an indicator of symbiont performance at maximal irradiance [31]. The near-zero values measured in this study suggest a high proportion of open

PSII reaction centers and possible light limitation. The plots in Fig 3 demonstrate that one of the three coral fragments tested in Tank 1 of Experiment 2 exhibited relatively low $\Delta F/F_m'_{,midday}$ and a higher Q_m (Fig 3; filled circles). In this case, the measuring head of the PAM fluorometer had inadvertently changed its position at the onset of the time series, so that it pointed towards the basal part instead of the growing coral apices of a coral branch. This basal part may have exhibited greater light scattering than the distal parts, which would explain the low $\Delta F/F_m'_{,midday}$ and higher Q_m [38]. This accidental observation emphasizes the importance of accurate placement of the measuring heads for measurement replication.

If we exclude these data for that reason, and consider each experiment separately, then it appears that $\Delta F/F_m'_{,midday}$ measured in ambient pCO_2 seawater (Control) was lower than that measured in CO_2-enriched seawater, in each of the three experiments. On the other hand, the midday excitation pressure, Q_m, was higher than that measured in CO_2-enriched seawater. Similar effects have been reported for *A. muricata* by Crawley et al. [20] and for *P. damicornis* by Jiang et al. [39], showing that CO_2 enrichment can decrease the PSII excitation pressure. In the former study, this decrease was caused by a reduction in F_v/F_m, while in the latter $\Delta F/F_m'$ increased, as observed in our study.

We also note that in Experiments 1 and 3, the slope of the $\Delta F/F_m'_{,midday}$ and $F_v/F_{m,19:00\ h}$ time series measured in increasingly CO_2 enriched seawater was smaller than that of the time series measured in ambient pCO_2 seawater (Fig 3). Similarly, the difference in the slope of the rETR/PAR relationship between Treatments and Control increased as the pCO_2 increased (Fig 4). This points to a possible positive effect of CO_2 enrichment; the increasing seawater pCO_2 may have counteracted the gradual decrease in $\Delta F/F_m'$ and rETR/PAR slope that was observed under ambient pCO_2 conditions. However, it remains unclear why such a trend was not observed in Experiment 2. If the coral fragments were to host different clades of

Symbiodinium, then this may explain a difference in response. However, since the fragments used in our experiment came from the same parental coral, this possibility seems unlikely.

We observed that under conditions of ambient pCO_2 $F_v/F_{m,19:00\ h}$ and $\Delta F/F_m'_{,midday}$ gradually decreased over time. Possible causes for this include incomplete acclimation to laboratory conditions. Before our experiment, the coral fragments lived in a constant 12/12 h dark/light regime with a PAR of approximately 90 μmol quanta m^{-2} s^{-1}, providing a daily photon flux of around 3.5 mol quanta m^{-2} day^{-1}. In our experiment, the PAR intensity was modulated around a midday peak, resulting in a smaller flux of 1.7–2.6 mol quanta m^{-2} day^{-1}. Although the coral *A. millepora* appears to tolerate low-light conditions [40,41], it seems that acclimation may take up to 20 days [40], which exceeds the acclimation period in our experiment. Seawater CO_2 enrichment may have supported such acclimation in Experiments 1 and 3 [20], preventing $\Delta F/F_m'_{,midday}$ of the coral fragments from decreasing as steeply as in the Control under conditions of ambient pCO_2.

The observed diurnal decline in $\Delta F/F_m'$ (Figs 2, S3) correlated with the daily peak in radiation exposure and possibly the development of reversible and photoprotective non-photochemical quenching [42,43]. On the other hand, the sharp decline in F_v/F_m during the night points to chlororespiration, which can create a trans-thylakoid $[H^+]$ gradient in the dark through cyclic electron transport around PSI, thereby promoting ATP production [44–46]. Chlororespiration requires oxygen and darkness or at least very low light [47]. In our experiment, these conditions were met at 18:30 h when PAR decreased below ~20 μmol quanta m^{-2} s^{-1} and was shut down at 19:00 h (S1 Fig 2).

Chlororespiration can deplete the accessible oxygen in the coral tissue [48,49]. Without an electron acceptor, electrons may have accumulated in the PSII–PSI electron transport chain, reducing the pool of plastoquinones. This will have initiated the transition of light harvesting complexes from PSII to PSI [44], decreasing the absorption cross section available for PSII

[50]. At dawn, F_v/F_m increased rapidly (Figs 2, S1 Fig 3) perhaps following the stimulation of PSI, which oxidized the plastoquinone pool and reversed the transition of light harvesting complexes [45]. Although the function of chlororespiration is still debated [44,51,52), its associated reduction of O_2 accumulated during the day may have lowered the risk of reactive oxygen damage to PSII, and the induced state transition may have supported an efficient onset of photosynthesis and O_2 production at the onset of light (44,53].

Conclusion

Our time series of saturation pulse analyses revealed evidence for chlororespiration of *Symbiodinium* sp. in the reef-building coral *A. millepora*. An inadvertent shift in the position of one of the PAM fluorometer measuring heads revealed differences between the basal part and the growing coral apices of a coral branch in $\Delta F/F_m'_{,midday}$ and Q_m—an accidental observation that emphasizes the importance of accurate sensor placement for measurement replication. Although two of three successive experiments indicated that CO_2 enrichment counteracted the gradual decrease in $\Delta F/F_m'_{,midday}$, $F_v/F_{m,19:00\ h}$, and the slope of the linear rETR/PAR regression, observed in the Control over the course of the experiment, statistical analyses failed to confirm such effect, rendering this experiment inconclusive. We believe that the possibility of such an effect warrants further experimentation.

Acknowledgments

Evan Brown assisted in the laboratory. Kim Currie, NIWA / University of Otago Research Centre for Oceanography, Dunedin, New Zealand, analyzed the seawater total alkalinity and dissolved inorganic carbon content. The constructive comments of Ian Hawes and Robin Hankin improved the clarity of the manuscript.

Author contributions

A.M. and K.V. conceived and performed the experiment and analyzed the data. K.V. wrote the paper with assistance from A.M. and D.B.

Data availability

The datasets are available from the corresponding author on reasonable request.

References

1. Doney SC, Fabry VJ, Feely RA, Kleypas JA. Ocean acidification: The other CO_2 problem. Ann Rev Mar Sci. 2009;6(1): 169–192.
2. Jokiel PL. The reef coral two compartment proton flux model: A new approach relating tissue-level physiological processes to gross corallum morphology. J Exp Mar Biol Ecol. 2011;409(1–2): 1–12.
3. Anthony KRN, Kline DI, Diaz-Pulido G, Hoegh-Guldberg O. Ocean acidification causes bleaching and productivity loss in coral reef builders. PNAS. 2008;105(45): 17442–17446.
4. Cohen AL, Holcomb M. Why corals care about ocean acidification: Uncovering the mechanism. Oceanography. 2009;22(4): 118–127.
5. Uthicke S, Fabricius KE. Productivity gains do not compensate for reduced calcification under near-future ocean acidification in the photosynthetic benthic foraminifer species *Marginopora vertebralis*. Glob Change Biol. 2012;18: 2781–2791.
6. Cyronak T, Schulz KG, Jokiel PL. The Omega myth: what really drives lower calcification rates in an acidifying ocean. ICES J Mar Sci. 2016;73: 558–562.
7. Bove CB, Davies SW, Ries JB, Umbanhowar J, Thomasson BC, Farquhar EB, et al. Global change differentially modulates Caribbean coral physiology. PLoS ONE. 2022;17(9): e0273897.
8. McCulloch MT, D'Olivo JP, Falter J, Holcomb M, Trotter JA. Coral calcification in a changing world and the interactive dynamics of pH and DIC upregulation. Nat Commun. 2017;8(1): 1–8.

9. Venn AA, Tambutté E, Holcomb M, Laurent J, Allemand D, Tambutté S. Impact of seawater acidification on pH at the tissue–skeleton interface and calcification in reef corals. PNAS 2013;110(5): 1634–1639.

10. Vidal-Dupiol J, Zoccola D, Tambutté E, Grunau C, Cosseau C, Smith KM, et al. Genes regulated to ion-transport and energy production are upregulated in response to CO_2-driven pH decreases in corals: new insights from transcriptome analysis. PLoS ONE 2013;8(3): e58652.

11. Muscatine L, Falkowski PG, Porter FW, Dubinsky Z. Fate of photosynthetic fixed carbon in light-and shade-adapted colonies of the symbiotic coral *Stylophora pistillata*. Proc Roy Soc Lond B Biol Sci. 1984;222(1227): 181–202.

12. Comeau S, Carpenter RC, Edmunds PJ. Coral reef calcifiers buffer their response to ocean acidification using both bicarbonate and carbonate. Proc Roy Soc Lond B Biol Sci 2013;280(1753): 20122374.

13. Tansik AL, Fitt WK, Hopkinson BM. Inorganic carbon is scarce for symbionts in scleractinian corals. Limnol Oceanogr. 2017;62(5): 2045–2055.

14. Enns T. Facilitation by carbonic anhydrase of carbon dioxide transport. Science 1967;155(3758): 44–47.

15. Al-Moghrabi S, Goiron C, Allemand D, Speziale N, Jaubert J. Inorganic carbon uptake for photosynthesis by the symbiotic coral-dinoflagellate association II. Mechanisms for bicarbonate uptake. J Exp Mar Biol Ecol. 1996;199(2): 227–248.

16. Rowan R, Whitney SM, Fowler A, Yellowlees D. Rubisco in marine symbiotic dinoflagellates: Form II enzymes in eukaryotic oxygenic phototrophs encoded by a nuclear multigene family. The Plant Cell 1996;8(3): 539–553.

17. Leggat W, Badger MR, Yellowlees D. Evidence for inorganic carbon-concentrating mechanism in the symbiotic dinoflagellate *Symbiodinium* sp. Plant Physiol. 1999;121(4): 1247–1255.

18. Oakley CA, Schmidt GW, Hopkinson BM. Thermal responses of *Symbiodinium* photosynthetic carbon assimilation. Coral Reefs 2014;33(2): 501–512.

19. Herfort L, Thanke B, Taubner I. Bicarbonate stimulation of calcification and photosynthesis in two hermatypic corals. J Phycol. 2008;44(1): 91–98.

20. Crawley A, Kline DI, Dunn S, Anthony KE, Dove S. The effect of ocean acidification on symbiont photorespiration and productivity in *Acropora formosa*. Glob Change Biol. 2010;16(2): 851–863.

21. Roberty S, Béraud E, Grover R, Ferrier-Pagès C. Coral productivity is co-limited by bicarbonate and ammonium availability. Microorganisms 2020;8(5): 640.

22. Noonan SH, Fabricius KE. Ocean acidification affects productivity but not the severity of thermal bleaching in some tropical corals. ICES J Mar Sci. 2016;73(3): 715–726.

23. Rodolfo-Metalpa R, Martin S, Ferrier-Pagès C, Gattuso JP. Response of the temperate coral *Cladocora caespitosa* to mid- and long-term exposure to pCO_2 and temperature levels predicted for the year 2100 AD. Biogeosciences 2009;7(1): 289–300.

24. Takahashi A, Kurihara H. Ocean acidification does not affect the physiology of the tropical *Acropora digitifera* during a 5-week experiment. Coral Reefs 2013;32(1): 305–314.

25. Hoadley KD, Pettay DT, Grottoli AG, Cai WJ, Melman TF, Schoepf V, et al. Physiological response to elevated temperature and pCO_2 varies across four Pacific coral species: Understanding the unique host+symbiont response. Sci Rep. 2015;5(1): 1–15.

26. Enochs IC, Derek P, Manzello DP, Carlton R, Schopmeyer S, Van Hooidonk R, Lirman D. Effects of light and elevated pCO_2 on the growth and photochemical efficiency of *Acropora cervicornis*. Coral Reefs 2014;33(2): 477–485.

27. Kaniewska P, Campbell PR, Kline DI, Rodriguez-Lanetty M, Miller D J, Dove S, Hoegh-Guldberg O. Major cellular and physiological impacts of ocean acidification on a reef building coral. PLoS ONE 2012;7(4): e34659.

28. Edmunds PJ. Effect of pCO_2 on the growth, respiration, and photophysiology of massive *Porites* spp. in Moorea, French Polynesia. Mar Biol. 2012;159(10): 2149–2160.

29. Bhagooli R, Mattan-Moorgawa S, Kaullysing D, Louis YD, Gopeechund A, Ramah S et al. Chlorophyll fluorescence – a tool to assess photosynthetic performance and stress photo-physiology in symbiotic marine invertebrates and seaplants. Mar Pollut Bull. 2021;165: 112059.

30. Kitajima MB, Butler WL. Quenching of chlorophyll fluorescence and primary photochemistry in chloroplasts by dibromothymoquinone. BBA–Bioenergetics 1975;376(1): 105–115.

31. Iglesias-Prieto R, Beltrán VH, LaJeunesse TC, Reyes-Bonilla H, Thomé PE. Different algal symbionts explain the vertical distribution of dominant reef corals in the eastern Pacific. Proc R Soc Lond Ser B. 2004;271: 1757–1763.

32. Klughammer C, Schreiber U. Complimentary PSII quantum yields calculated from simple fluorescence parameters measured by PAM fluorometry and the saturation pulse method. PAM Application Notes 2008;1(2): 201–247.

33. Dickson AG, Sabine CL, Christian JR. Guide to best practices for ocean CO_2 measurements: PICES Special Publication 3. 2007. http://cdiac.ornl.gov/oceans/Handbook_2007.html

34. Lewis E, Wallace DWR. Program developed for CO_2 system calculations. ORNL/CDIAC-105. Carbon Dioxide Information Analysis Center, Oak Ridge National Laboratory, U.S. Department of Energy, Oak Ridge, Tennessee, 1998

35. Dickson AG (). Standard potential of the reaction: $AgCl_{(s)} + 12H_{2(g)} = Ag_{(s)} + HCL_{(aq)}$, and the standard acidity constant of the ion HSO_4^- in synthetic seawater from 273.15 to 318.15 K. J Chem Thermodyn. 1990;22: 113–127.

36. Mehrbach C, Culberson CH, Hawley JE, Pytkowicz RN. Measurement of the apparent dissociation constants of carbonic acid in seawater at atmospheric pressure. Limnol Oceanogr. 1973;18: 897–907.

37. Dickson AG, Millero FJ. A comparison of the equilibrium constants for the dissolution of carbonic acid in seawater media. Deep Sea Res. 1987;34(10): 1733–1743.

38. Enriquez S, Méndez ER, Iglesias-Prieto R. Multiple scattering on coral skeletons enhances light absorption by symbiotic algae. Limnol Oceanogr. 2005;50: 1025–1032.

39. Jiang L, Guo YJ, Zhang YY, McCook LJ, Yuan XC, Lei XM, et al. Diurnally fluctuating pCO_2 modifies the physiological responses of coral recruits under ocean acidification. Front Physiol. 2019;9: 1952.

40. DiPerna S, Hoogenboom M, Noonan S, Fabricius K. Effects of variability in the daily light integrals on the photophysiology of the corals *Pachyseris speciosa* and *Acropora millepora*. PLoS ONE 2018;13(9): e0203882.

41. Kuanui P, Chavanich S, Viyakarn V, Omori M, Fujita T, Lin C. Effect of light intensity on survival and photosynthetic efficiency of cultured corals of different ages. Estuar Coast Shelf Sci. 2020;235: 106515.

42. Ralph PJ, Gademann R, Larkum AWD, Schreiber U. In situ underwater measurements of photosynthetic activity of coral zooxanthellae and other reef-dwelling dinoflagellate endosymbionts. Mar Ecol Prog Ser. 1999;180: 139–147.

43. Gorbunov MY, Kolber ZS, Lesser MP, Falkowski PG. Photosynthesis and photoprotection in symbiotic corals. Limnol Oceanogr. 2001;46: 75–85.

44. Jones RJ, Hoegh-Guldberg O. Diurnal changes in the photochemical efficiency of the symbiotic dinoflagellates (Dinophyceae) of corals: photoprotection, photoinactivation and the relationship to coral bleaching. Plant Cell Environ. 2001;24(1): 89–99.

45. Hill R, Ralph PJ. Diel seasonal changes in fluorescence rise kinetics of three scleractinian corals. Funct Plant Biol. 2005;32: 549–559.

46. Rumeau D, Peltier G, Cournac L. Chlororespiration and cyclic electron flow around PSI during photosynthesis and plant stress response. Plant Cell Environ. 2007;30(9): 1041–1051.

47. Bennoun P. Chlororespiration revisited: mitochondrial-plastid interactions in *Chlamydomonas*. BBA–Bioenergetics. 1994;1186(1–2): 59–66.

48. Shashar N, Cohen Y, Loya Y. Extreme diel fluctuations of oxygen in diffusive boundary layers surrounding stony corals. Biol Bull. 1993;185(3): 455–461.

49. Kühl M, Cohen Y, Dalsgaard T, Jørgensen BB, Revsbech NP. Microenvironment and photosynthesis of zooxanthellae in scleractinian corals studied with microsensors for O_2, pH and light. Mar Ecol Prog Ser. 1995;117(1–3): 159–172.

50. Warner ME, Berry-Lowe S. Differential xanthophyll cycling and photochemical activity in symbiotic dinoflagellates in multiple locations of three species of Caribbean coral. J Exp Mar Biol Ecol. 2006;339(1): 86–95.

51. Nixon PJ. Chlororespiration. Philos Trans R Soc Lond B: Biol Sci. 2000;355(1402): 1541–1547.

52. Hill R, Ralph PJ. Dark-induced reduction of the plastoquinone pool in zooxanthellae of scleractinian corals and implications for measurements of chlorophyll a fluorescence. Symbiosis 2008;46(1): 45–56.

53. Norrick WJ, Buchert F, Joliot P, Rappaport F, Bailleul B, Wollman FA. Chlororespiration controls growth under intermittent light. Plant Physiol. 2019;179(2): 630–639.

54. Schreiber U, Endo T, Mi H, Asada K. Quenching analysis of chlorophyll fluorescence by the saturation pulse method: Particular aspects relating to the study of eukaryotic algae and cyanobacteria. Plant and Cell Physiology 1995;36(5): 873–882.